Aurora B and condensin are dispensable for chromosome arm and telomere separation during meiosis II

Julien Berthezene, Céline Reyes, Tong Li, Stephane Coulon, Pascal Bernard, Yannick Gachet, Sylvie Tournier

Aurora B and condensin are dispensable for chromosome arm and telomere separation during meiosis II

Julien Berthezene[a], Céline Reyes[a], Tong Li[a], Stéphane Coulon[b], Pascal Bernard[c,d], Yannick Gachet[a,*], and Sylvie Tournier[a,*]

[a]LBCMCP, Centre de Biologie Intégrative, Université de Toulouse, CNRS, UPS, 31062 Toulouse, France; [b]CNRS, INSERM, Aix Marseille Univ, Institut Paoli-Calmettes, CRCM, 13273 Marseille, France; [c]CNRS—Laboratory of Biology and Modelling of the Cell, UMR 5239, 69364 Lyon, France; [d]ENS de Lyon, Université Lyon, F-69007 Lyon, France

ABSTRACT **In mitosis, while the importance of kinetochore (KT)-microtubule (MT) attachment has been known for many years, increasing evidence suggests that telomere dysfunctions also perturb chromosome segregation by contributing to the formation of chromatin bridges at anaphase. Recent evidence suggests that Aurora B kinase ensures proper chromosome segregation during mitosis not only by controlling KT-MT attachment but also by regulating telomere and chromosome arm separation. However, whether and how Aurora B governs telomere separation during meiosis has remained unknown. Here, we show that fission yeast Aurora B localizes at telomeres during meiosis I and promotes telomere separation independently of the meiotic cohesin Rec8. In meiosis II, Aurora B controls KT-MT attachment but appears dispensable for telomere and chromosome arm separation. Likewise, condensin activity is nonessential in meiosis II for telomere and chromosome arm separation. Thus, in meiosis, the requirements for Aurora B are distinct at centromeres and telomeres, illustrating the critical differences in the control of chromosome segregation between mitosis and meiosis II.**

Monitoring Editor
Kerry Bloom
University of North Carolina, Chapel Hill

Received: Jan 9, 2020
Revised: Feb 13, 2020
Accepted: Feb 18, 2020

INTRODUCTION

In eukaryotes, accurate chromosome segregation during mitosis relies on the migration of sister chromatids toward the opposite poles of the mitotic spindle. To achieve correct chromosome segregation, kinetochores (KTs), multiprotein complexes assembled at centromeres, must interact with microtubules (MTs). When sister KTs are captured by MTs coming from opposite poles of the mitotic spindle, the mitotic chromosome becomes bilaterally attached and congresses toward the spindle equator. At anaphase, sister chromatids separate and move toward the poles due to the proteolytic cleavage of cohesin, which ensures sister chromatid cohesion (Uhlmann *et al.*, 1999). Sister chromatid cohesion defines the correct back-to-back arrangement of sister KTs and prevents chromosome attachment defects such as merotelic attachment, in which one KT is attached to both poles (Gregan *et al.*, 2007, 2011; Courtheoux *et al.*, 2009; Sakuno *et al.*, 2009). The stiffness of chromosome arms, conferred by condensin, transmits the traction forces exerted on centromeres by MTs throughout chromosome arms up to the telomeres, allowing the full separation of chromosomes (Renshaw *et al.*, 2010). Spindle lengthening (anaphase B) further separates the two sets of chromosomes, and cytokinesis ensures a complete partitioning of the two daughter cells.

It is crucial for the accurate segregation of chromosomes that cohesion is not destroyed until all chromosomes are bilaterally attached to the mitotic spindle. This key coordination is ensured by an error detection and correction system, which involves Aurora B kinase (Chan and Botstein, 1993; Lampson and Cheeseman, 2011) and the spindle assembly checkpoint (SAC) (Rieder *et al.*, 1995; Rudner and Murray, 1996; Cleveland *et al.*, 2003). Aurora B and SAC

This article was published online ahead of print in MBoC in Press (http://www.molbiolcell.org/cgi/doi/10.1091/mbc.E20-01-0021) on February 26, 2020.

The authors declare no competing financial interests.

*Address correspondence to: Sylvie Tournier (sylvie.tournier-gachet@univ-tlse3.fr); Yannick Gachet (yannick.gachet@univ-tlse3.fr).

Abbreviations used: CPC, chromosomal passenger complex; KT, kinetochore; MT, microtubule; SAC, spindle assembly checkpoint; SPB, spindle pole body.

components operate at the level of KTs and monitor chromosome attachment, allowing the destabilization of erroneous attachments. Aurora B destabilizes faulty KT-MT attachments through the phosphorylation of key KT substrates (Tanaka *et al.*, 2002; Cimini *et al.*, 2006; Kelly and Funabiki, 2009). In anaphase, correction of attachment defects by Aurora B is dependent on forces generated at the spindle midzone during spindle elongation (Courtheoux *et al.*, 2009; Gay *et al.*, 2012). In addition, Aurora B regulates key mitotic and meiotic events such as condensin binding and chromosome condensation, chromosome orientation, central spindle formation, and the regulation of furrow ingression and abscission (Sampath *et al.*, 2004; Kotwaliwale *et al.*, 2007; Mora-Bermudez *et al.*, 2007; Steigemann *et al.*, 2009; Tada *et al.*, 2011; Meyer *et al.*, 2013). Aurora B is the catalytic subunit of the chromosomal passenger complex (CPC). In *Schizosaccharomyces pombe*, components of the CPC, Bir1/Survivin, Pic1/INCENP, Nbl1/Borealin, and Ark1/Aurora B are major regulators of mitosis (Morishita *et al.*, 2001; Petersen *et al.*, 2001; Leverson *et al.*, 2002). Inhibition of Aurora B using a Shokat analog-sensitive mutant leads to chromosome segregation defects (Hauf *et al.*, 2007; Gay *et al.*, 2012). Several mitotic substrates of Aurora B have been identified (Koch *et al.*, 2011; Carmena *et al.*, 2012). Notably, Aurora B regulates the binding of condensin to chromosomes in a wide range of systems (Giet and Glover, 2001; Morishita *et al.*, 2001; Ono *et al.*, 2004). In fission yeast, Aurora B-dependent phosphorylation of Cnd2, the kleisin subunit of condensin, promotes condensin recruitment to chromosomes (Nakazawa *et al.*, 2011; Tada *et al.*, 2011). Similarly, in human cells, phosphorylation of the kleisin CAP-H by Aurora B promotes efficient association of condensin I to mitotic chromosomes (Ono *et al.*, 2004; Lipp *et al.*, 2007; Tada *et al.*, 2011).

In line with its wide range of functions, Aurora B exhibits a dynamic localization during the cell cycle. Aurora B concentrates at the inner centromeric chromatin in metaphase and eventually relocalizes at the spindle midzone during anaphase (Petersen *et al.*, 2001). Aurora B has also been observed at telomeres during mitosis (Vanoosthuyse *et al.*, 2007; Yamagishi *et al.*, 2010; Reyes *et al.*, 2015). Recent studies described a key role for Aurora B as a regulator of telomere structural integrity. In mammalian cells, loss of Aurora B function affects TERF1/TRF1 (a component of the telomeric Shelterin complex) resulting in aberrant telomere structure (Chan *et al.*, 2017). Aurora B also regulates an active telomere conformational change from looped to linear during mitotic arrest coincident with ATM-dependent telomere DNA damage response activation (Van Ly *et al.*, 2018). Moreover, it has been proposed that mammalian telomeres exist in an underprotected state during mitosis due to an Aurora B-dependent effect on the telomeric Shelterin complex (Hayashi *et al.*, 2012; Orthwein *et al.*, 2014).

We previously identified a Telomere Disjoining Pathway that governs the efficient separation of chromosome ends during mitosis, which involves an Aurora–B-dependent cascade of events at fission yeast telomeres (Reyes *et al.*, 2015). In mitosis, the physical separation of telomeres is a tightly regulated, two-step process, which relies on telomeric proteins, condensin and Aurora B kinase. Aurora B primes telomeres for separation in metaphase by delocalizing several proteins including Shelterin, Swi6^{HP1}, and cohesin, and it promotes telomere separation in anaphase by facilitating condensin loading (Reyes *et al.*, 2015).

The emerging roles of Aurora B in mitosis at those chromosomal loci, that is, telomeres and chromosome arms, prompted us to investigate the function of this kinase during the meiotic process. Indeed, meiosis represents an attractive model in which to study the intricate relationship among telomeres, condense, and Aurora B since it involves a single round of DNA replication followed by two series of chromosome segregation. Meiosis I relies on the pairing of replicated homologous chromosomes and on the pulling of pairs of homologous sister centromeres in opposite directions, while in meiosis II, sister centromeres split as they do in mitosis. In addition, during meiosis, telomeres exhibit critical and striking features. In premeiotic S-phase, chromosomes reorganize to form the bouquet configuration where telomeres are arranged as a large cluster beneath the spindle pole body (SPB; Chikashige *et al.*, 1994; Scherthan, 2001). This telomere cluster is tightly anchored to the nuclear envelope (Chikashige *et al.*, 2006; Hiraoka and Dernburg, 2009). Previous studies in *S. pombe* have established that the telomere bouquet has crucial functions in the preparation of meiotic chromosome segregation. These functions encompass promoting homologous chromosome recombination (Cooper *et al.*, 1998), setting up spindle formation (Tomita and Cooper, 2007), participating in meiotic centromere assembly (Klutstein *et al.*, 2015), and finally controlling prophase progression and exit (Moiseeva *et al.*, 2017).

In the present study, we used live single cell imaging to analyze centromere, telomere, and chromosome arm separation when Aurora B or condensin was selectively inactivated in meiosis I or meiosis II. We demonstrate that the activity of Aurora B and condensin is required for telomere and chromosome arm separation in meiosis I but not in meiosis II. We further show that the functions of Aurora B in KT-MT attachment and telomere separation can be distinguished. Finally, our study also suggests the existence of a noncanonical mechanism to segregate chromosome arms in meiosis II when Aurora or condensin is inactivated.

RESULTS

Telomere separation is a two-step process in meiosis I as opposed to meiosis II

To investigate the mechanisms controlling telomere separation in meiosis, we performed live imaging of cells expressing a SPB marker, Cdc11-CFP (Tournier *et al.*, 2004), and a telomere marker protein, Taz1-GFP; a homologue of mammalian TRF1/TRF2 that binds to telomere repeats (Cooper *et al.*, 1997; Vassetzky *et al.*, 1999; Chikashige and Hiraoka, 2001) (Figure 1).

Fission yeast has three chromosomes for 12 telomeres in mitosis. At the beginning of meiosis, during the horse-tail movement, the 24 telomeres are organized in clusters at the SPBs while the centromeres are positioned away from the SPBs (bouquet conformation). We followed individual *taz1-gfp cdc11-cfp* cells through meiosis I (Figure 1, A–C). In early meiosis I, a short spindle (up to 3.0 μm) is formed, as judged by SPB separation. A second phase (from 3 to 5.0 μm) is observed where spindle length is roughly maintained until full separation of homologous chromosomes (anaphase A). The third phase of meiosis I consists entirely of anaphase B, during which the spindle elongates along the long axis of the cell (Supplemental Figure S1A; Supplemental Movie S1). Telomeres separate in two steps during meiosis I. First, telomere cluster dispersion is initiated in early meiosis I prior to anaphase A (from 1 to 12 foci; spindle size from 0 to 5 μm), and second, clusters fully dissociate during anaphase B when chromosome arms separate (telomere disjunction, from 10 to 20 foci, spindle size from 5 to 15 μm; Supplemental Movie S1). An example of meiosis I telomere dispersion and disjunction is shown in a single cell analysis (Figure 1B) together with a quantification of Taz1 foci during meiotic progression in multiple individual meiotic cells (Figure 1C) confirming that telomere separation is a two-step process. Importantly, during prophase of meiosis II, telomeres were able to form new clusters (Supplemental Figure S1B). Quantification of Taz1 focus number and position confirmed

that the reestablishment of telomere clusters and their relocalization to the nuclear periphery occur after spindle disassembly in prophase II before the onset of metaphase II (Supplemental Figure S1C).

We similarly analyzed telomere separation during meiosis II (Figure 1, D–F). In early meiosis II, two short spindles are formed (up to 2.0 µm), as judged by SPB separation. A second phase (from 2 to 3.0 µm) is observed where both spindles roughly maintained the same size until sister chromatids separate (anaphase A). The third phase consists of anaphase B, during which the two spindles moderately elongate within the cell (up to 10 µm) (Supplemental Figure S1A; Supplemental Movie S2). An example of meiosis II telomere dissociation is shown in a single cell analysis (Figure 1E) together with a quantification of Taz1 foci during meiosis II progression in several cells (Figure 1F). Interestingly, we observed a single step in telomere separation, which was mostly achieved in metaphase II, that is, prior to the full separation of sister chromatids in anaphase II (Figure 1, E and F). Quantification of Taz1 foci confirmed the reestablishment of telomere clusters during spore formation (Supplemental Figure S1B).

Together, these experiments demonstrate that telomere clustering is highly regulated throughout the meiotic cell cycle and while telomere dissociation is a two-step process in meiosis I, it occurs in a single phase in meiosis II.

Aurora B kinase controls telomere and chromosome arm separation in meiosis I but not in meiosis II

To test whether Aurora B plays a role in telomere separation in meiosis, we used ATP analog-sensitive alleles of Aurora B (Shokat mutant *ark1-as3*) (Hauf *et al.*, 2007). Aurora B activity was specifically inhibited in meiosis I or meiosis II (see *Materials and Methods*) by adding the nonhydrolizable ATP analog 1-NA-PP1 (10 µM). Meiotic progression of *ark1-as3* cells expressing telomere *(taz1-gfp,* green) and SPB markers (*cdc11-cfp,* red) was recorded 10 min after adding the inhibitor (Figure 2). In meiosis I, single cell analysis of the number of Taz1 foci with respect to spindle size reveals that Aurora B inhibition significantly perturbed telomere separation and even promoted reclustering of telomeres in anaphase I after full spindle elongation (Figure 2, A–C; Supplemental Movie S3). Thus, in addition to its previously described role at centromeres in the correction of faulty KT-MT attachment (Supplemental Figure S2, A–C), Aurora B is required in meiosis I for telomere separation.

In this set of experiments, we noticed that when Aurora inhibition was conducted from the beginning of meiosis I, the onset of meiosis II was also deeply perturbed because of spindle collapse occurring in meiosis I (not shown). Thus, to specifically analyze the role of Aurora B during meiosis II, we added the inhibitor 1-NA-PP1 to *ark1-as3 taz1-gfp cdc11-cfp* cells only during prophase II and followed cells progressing into meiosis II (see *Materials and Methods*; Figure 2, D–F). An example of telomere separation during meiosis II when Aurora is inhibited is shown in a single cell analysis (Figure 2, D and E; Supplemental Movie S4) together with a quantification of Taz1 foci during meiosis II progression in multiple cells (Figure 2F). Surprisingly, when Aurora was inhibited specifically in meiosis II, the kinetic of telomere separation remained unchanged. Telomeres appeared clustered during metaphase II and fully separated at the anaphase II transition (Figure 2, E and F). This observation was not due to the lack of efficiency of Aurora inhibition since we found that centromere segregation was greatly impacted by Aurora inhibition in meiosis II (Supplemental Figure S2, D and E). Accordingly, using histone H3-mRFP (red) and Taz1-GFP (green) markers, we observed that Aurora inhibition blocked the separation of chromosome arms and telomeres in meiosis I (Figure 3, A and B). In sharp contrast, although lagging chromosomes were present, chromosome arms and telomeres successfully separated during anaphase II despite the inhibition of Aurora B (Figure 3, C and D).

To better understand the differences between Aurora's role in equational (meiosis II) versus reductional (meiosis I) chromosome segregation, we performed imaging of live cells simultaneously expressing markers for the SPBs-KTs (Cdc11-CFP, Ndc80-CFP, blue), telomeres (Taz1-RFP, red), and Aurora B (Ark1-GFP, green) (Figure 4). In addition to its well-known localization at KTs and the spindle midzone in metaphase of meiosis I and II (Petersen *et al.*, 2001; Hauf *et al.*, 2007), we observed that Aurora B also colocalizes transiently to telomeres in metaphase of meiosis I (Figure 4, A and B). Intriguingly, telomere localization of Aurora B was exclusively seen in meiosis I but not in meiosis II (Figure 4A). In addition, telomere localization of Aurora in meiosis I rapidly vanished at the metaphase to anaphase transition in parallel with telomere disjunction (Figure 4C; Supplemental Figure S3).

In conclusion, Aurora B activity is required for proper KT-MT attachment and telomere and chromosome arm separation in meiosis I. Conversely, in meiosis II, Aurora B activity is dispensable for telomere and chromosome arm separation, though it remains necessary for correct KT-MT attachment. Moreover, the role of Aurora in telomere/chromosome arm separation correlates with its localization to telomeres, as previously observed during mitosis (Reyes *et al.*, 2015).

Aurora controls condensin localization to chromosome arms in meiosis I and meiosis II

In fission yeast, the Aurora B-dependent phosphorylation of the kleisin Cnd2 during mitosis promotes condensin recruitment to chromosomes (Nakazawa *et al.*, 2011; Tada *et al.*, 2011). To determine whether this mechanism was also conserved in meiosis, we performed imaging of living cells simultaneously expressing markers for the SPBs (Cdc11-CFP, red) and the condensin subunit Cnd2 (Cnd2-GFP, green) before or after Aurora inhibition (Figure 5). As previously described in mitosis (Nakazawa *et al.*, 2008), we observed that condensin localizes in meiosis I to several nuclear foci compartments, possibly corresponding to nucleolar or KT foci (Figure 5A, left panel; Supplemental Movie S5). At anaphase onset, condensin switches to the spindle midzone (white arrow) and chromosome arms (yellow arrows) but foci largely disappear. A histogram analysis of foci pixel intensities of condensin localization during meiosis I progression confirms the reorganization of condensin localization during meiotic progression (Figure 5C, left panel).

Similarly to what has been described in mitosis (Nakazawa *et al.*, 2011; Tada *et al.*, 2011), the presence of condensin foci in metaphase of meiosis I was clearly reduced after Aurora inhibition (Figure 5A, right panel; Supplemental Movie S6). Consistent with this, the histogram analysis of foci pixel intensities following Aurora inhibition remained low from prophase to anaphase (Figure 5C, right panel). A similar analysis of condensin localization in meiosis II again revealed the presence of several nuclear foci in metaphase. At anaphase II onset, condensin switches to chromosome arms (yellow arrows) and the spindle midzone (white arrows) (Figure 5B, left panel; Supplemental Movie S7). Following Aurora inhibition, we observed the complete extinction of the chromosomal localization of condensin in anaphase II (Figure 5B, right panel; Supplemental Movie S8) and only spindle midzone (white arrows) condensin signal remained present.

Thus, Aurora B controls formation of nuclear condensin foci in meiosis I and meiosis II as previously reported in mitosis. However, the function of Aurora B is only essential for chromosome arms and telomere separation in meiosis I but dispensable in meiosis II.

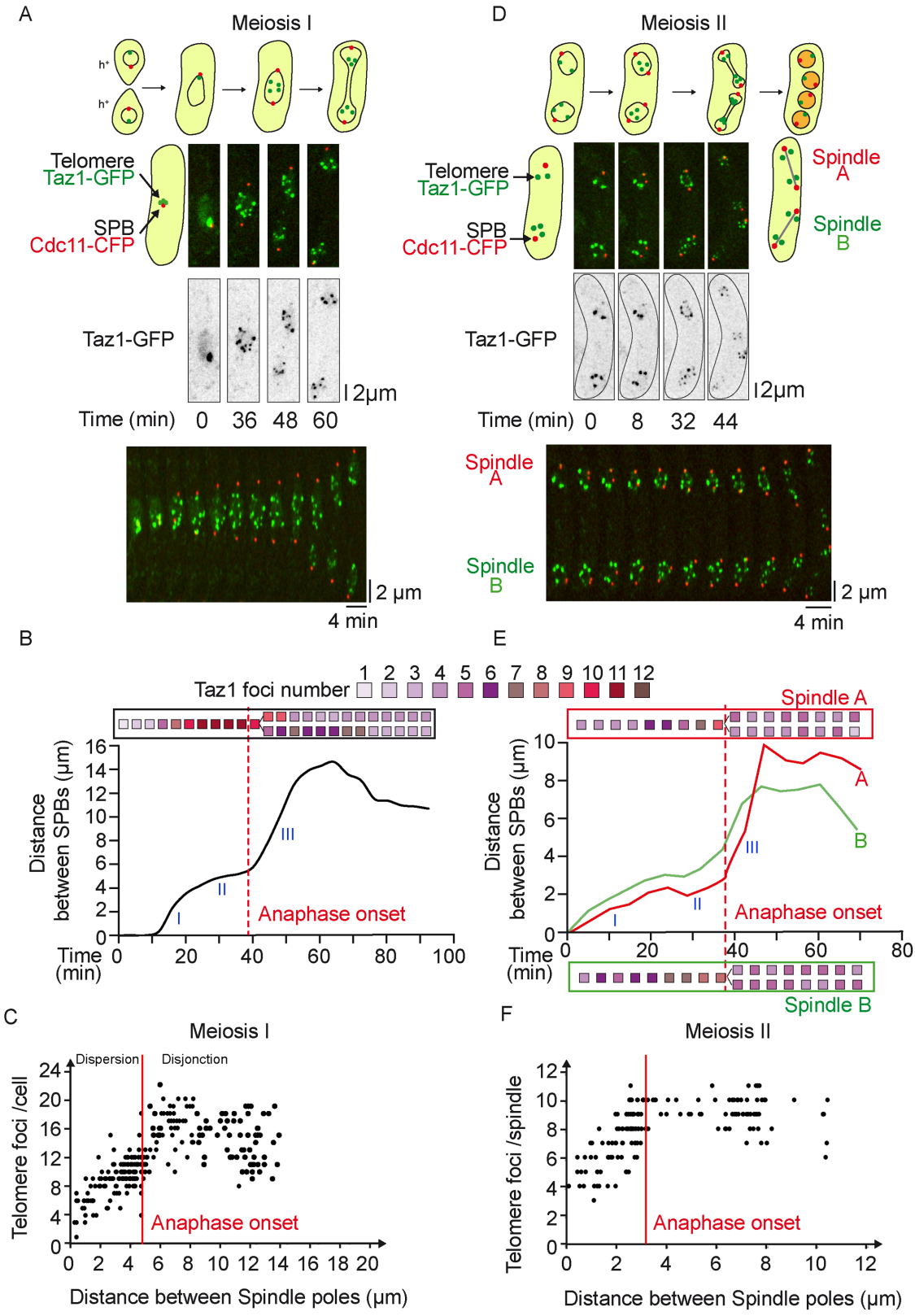

FIGURE 1: Telomere cluster dissociation occurs in two steps in meiosis I but in a single step during metaphase of meiosis II. (A) Selected frames from a movie of a live cell undergoing meiosis I. Telomeres are visualized via Taz1-GFP (green) and SPBs via Cdc11-CFP (red). (B) Telomere foci dynamics during meiosis I. A kymograph and analysis of the movie shown in A are presented. The number of telomere foci is shown with a color code for each frame of the movie. After anaphase I onset, telomere foci numbers were counted separately in both sets of segregated chromosomes. (C) Number of telomere foci according to the distance between SPB foci. Data were measured on static images of cells ($n = 264$) in meiosis I. Characteristic spindle length of anaphase I onset was estimated to be in average

Aurora B phosphorylation of condensin promotes chromosome arm/telomere separation in meiosis I

Previous studies in fission yeast have established that Cnd2 is a mitotic Aurora B substrate (Nakazawa *et al.*, 2011; Tada *et al.*, 2011), and a Cnd2 phosphomimetic mutant (*cnd2-3E*) alleviates chromosome segregation defects in cells where Aurora B has been inactivated (Nakazawa *et al.*, 2011; Tada *et al.*, 2011; Reyes *et al.*, 2015). We speculated that phosphorylation of Cnd2 by Aurora B may also be sufficient to promote telomere dissociation and chromosome arm separation in meiosis I. To address this point, we used *cnd2-3E ark1-as3* mutant cells that also expressed SPB (Cdc11-cfp, red) and telomere (Taz1-gfp, green) markers. We scored the number of Taz1 foci relative to spindle length in *cnd2-3E* cells after Aurora inhibition in meiosis I (Figure 6, A–C). As shown in Figure 6C, the *cnd2-3E* mutant completely bypassed the telomere nondisjunction phenotype that arises from Aurora inhibition in meiosis I. Similarly and as expected, inhibiting Aurora in meiosis II in a *cnd2-3E* mutant had no impact on telomere dissociation (Figure 6, D–F). However, contrary to what has been observed in mitosis (Reyes *et al.*, 2015), the *cnd2-3E* mutation did not alleviate the centromere attachment defects after Aurora B inactivation (Supplemental Figure S4). Indeed, *cnd2-3E* cells displayed numerous lagging and missegregated centromeres following Aurora inhibition (Supplemental Figure S4). This syntelic attachment phenotype is also confirmed in Figure 6, A and B, since a different number of telomeres is observed in the two daughter cells. Similarly, in meiosis II, while the effect of Aurora on telomere separation in this mutant was undistinguishable from control cells (Figure 6, D–F), Aurora's role at centromeres, visualized through the presence of lagging and centromere missegregation, was independent of Cnd2 phosphorylation (Supplemental Figure S4).

Together, these observations suggest that Aurora B controls telomere and chromosome arm separation, through phosphorylation of the condensin Cnd2 subunit in meiosis I but not in meiosis II. As opposed to mitosis, Aurora's role in correcting centromere attachment is largely but not totally independent of Cnd2 phosphorylation in meiosis I and II.

Condensin is required for telomere and chromosome arm separation in meiosis I but not meiosis II

Our observations suggest that the activity of the condensin complex may be dispensable for telomere and chromosome arm separation in meiosis II. To verify this, we expressed SPB (Cdc11-CFP, red) and telomere (Taz1-GFP, green) markers cells bearing a conditional shut-off allele for the condensin subunit $Cut14^{Smc2}$ (combining promoter repression with an auxin-inducible degron) (Kakui *et al.*, 2017). To determine the effect of condensin degradation on chromosome arm and telomere separation, we analyzed the number of telomere foci with respect to spindle size in meiosis I and II (Figure 7, A–C). In meiosis I, even after full spindle elongation, the number of telomere foci was significantly reduced when condensin was degraded (Figure 7, A and B). This phenotype was similar to Aurora inhibition. However, in contrast to our observations following Aurora inhibition, condensin degradation led to few centromeric segregation defects (Supplemental Figure S4). Similarly, we addressed the role of Condensin in meiosis II by inducing condensin depletion (see *Materials and Methods*; Figure 7, A–D). Interestingly, telomere and chromosome arm separation in anaphase II was not deeply impeded by condensin degradation (Figure 7, A and C). To further analyze the role of Aurora and condensin in chromosome arm condensation, we measured the distance between individual telomeres and the closest SPB during meiosis II progression. Indeed, in comparison to budding yeast chromosomes, the three chromosomes of fission yeast are considerably longer. Taking advantage of these long chromosomes, Petrova *et al.* previously established a chromosome condensation assay that measures distances between fluorescently labeled loci in live fission yeast cells (distance between chromosome arm loci to centromeres) (Petrova *et al.*, 2013). Based on this method, we chose to measure the distance from telomeres to SPBs. As expected, condensin degradation and Aurora inhibition caused chromosome arm condensation defects in anaphase of meiosis II as judged by the increase in SPB to telomere distances (Figure 7D; spindle size between 5 and 8 μm). Notably, the defect in chromosome arm condensation following Aurora inhibition was bypassed in the *cnd2-3E* phosphomimetic mutant (Figure 7D). However, at the end of meiosis II (postelongation constant spindle size), chromosome arms were able to separate as judged by the decreasing distance between the SPBs and the telomeres (Figure 7D), although we could confirm that the localization of Cnd2-GFP was affected by the degradation of Cut14 (condensin complex Smc2 subunit) both in meiosis I and II (Figure 8, A and B).

These observations confirm that telomere/chromosome arm separation requires condensin function in meiosis I but not in meiosis II. Furthermore, both in meiosis I and meiosis II, the importance of condensin in the control of KT-MT attachment remains limited.

Therefore, these results suggest the existence of an Aurora- and condensin-independent mechanism to separate chromosome arms in meiosis II.

Role of meiotic or mitotic cohesins in Aurora's function at telomere/chromosome arms

It has been suggested that new cohesion on chromosome arms cannot be generated between meiosis I and II in the absence of de novo DNA replication (Uhlmann and Nasmyth, 1998; Toth *et al.*, 1999; Watanabe and Nurse, 1999; Watanabe *et al.*, 2001). We thus hypothesized that the phenotypic differences observed between meiosis I and II, when Aurora is inhibited, could be due to the presence of cohesin on chromosome arms. We tested the role of cohesin in the chromosome arm/telomere phenotypes observed following Aurora inhibition. During meiosis I, cohesion is eliminated along chromosome arms to allow homologous segregation, but persists between sister centromeres moving toward the same spindle pole. The fission yeast cohesin protein Rec8 plays a key role in this process. Rec8 largely localizes all along chromosomes and persists at the centromeric regions throughout meiosis I until the anaphase of meiosis II (Watanabe and Nurse, 1999). To test whether Aurora B's role in telomere and chromosome arm separation was dependent

of 5 μm. (D) Selected frames from a movie of a live cell undergoing meiosis II. Telomeres are visualized via Taz1-GFP (green) and SPBs via Cdc11-CFP (red). (E) Telomere foci dynamics during meiosis II. A kymograph and analysis of the movie shown in D are presented; the top and bottom meiosis II spindles of the movie are defined as spindle A and spindle B, respectively. The number of telomere foci is shown with a color code for each frame of the movie for both Spindle A (red box) and Spindle B (green box). After anaphase II onset, telomere foci numbers were counted separately for both sets of segregated chromosomes. (F) Number of telomere foci according to the distance between SPB foci. Data were measured from meiosis II movies ($n = 12$). Characteristic spindle length of anaphase II onset was estimated at 3.2 μm.

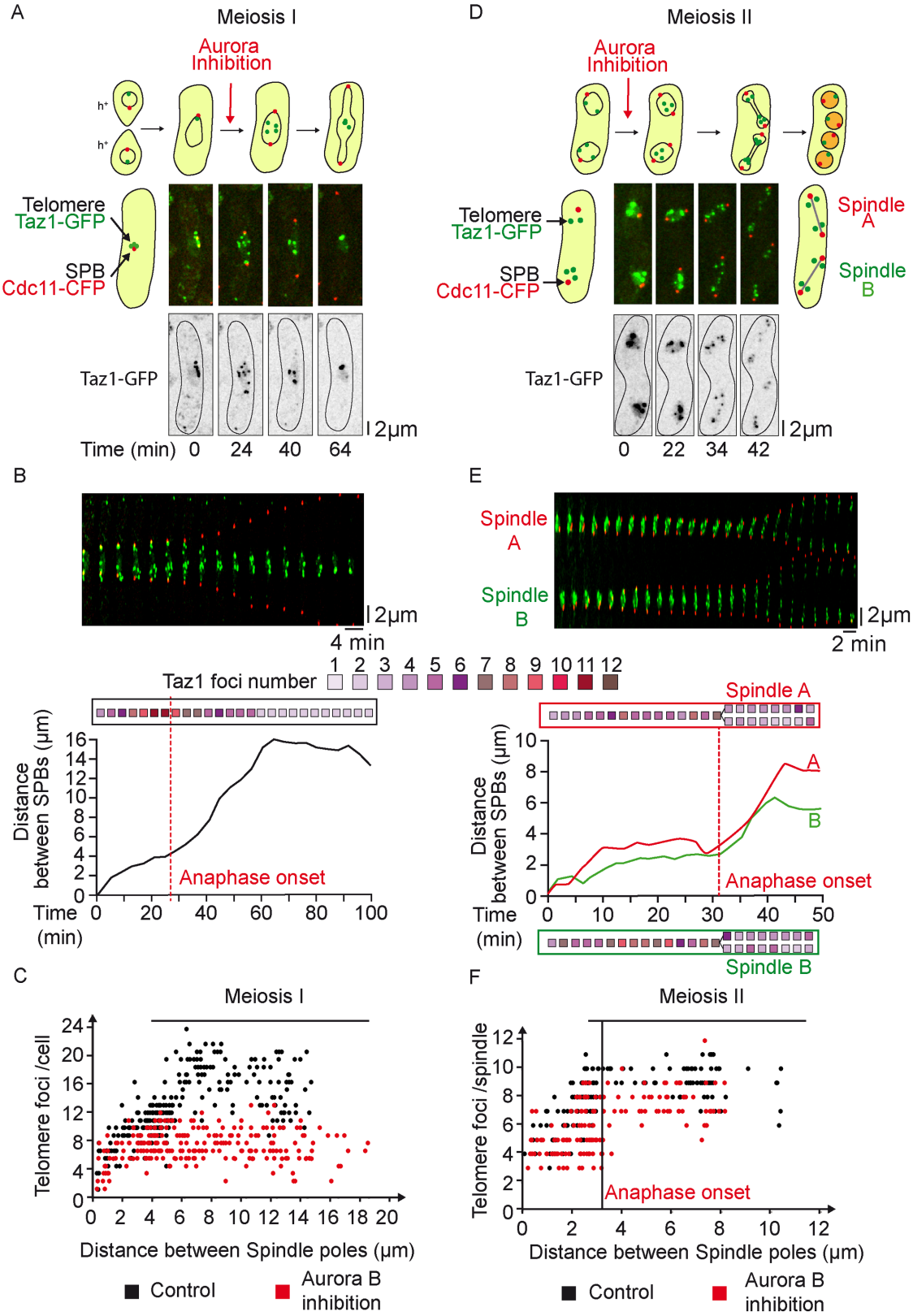

FIGURE 2: Aurora kinase function is required for the separation of telomeres in meiosis I but is dispensable in meiosis II. (A) Selected frames from a live *ark1-as3* cell undergoing meiosis I under Aurora inhibition. Aurora inhibition is performed by exposure of an *ark1-as3* cell to 10 μM 1-NA-PP1. Telomeres are visualized via Taz1-GFP (green) and SPBs via Cdc11-CFP (red). (B) Telomere foci dynamics during meiosis I under Aurora inhibition. A kymograph and analysis of the movie shown in A is presented. The number of telomere foci is shown with a color code for each frame of the movie. After anaphase I onset, telomeres do not separate and instead gradually reform clusters. (C) Number of

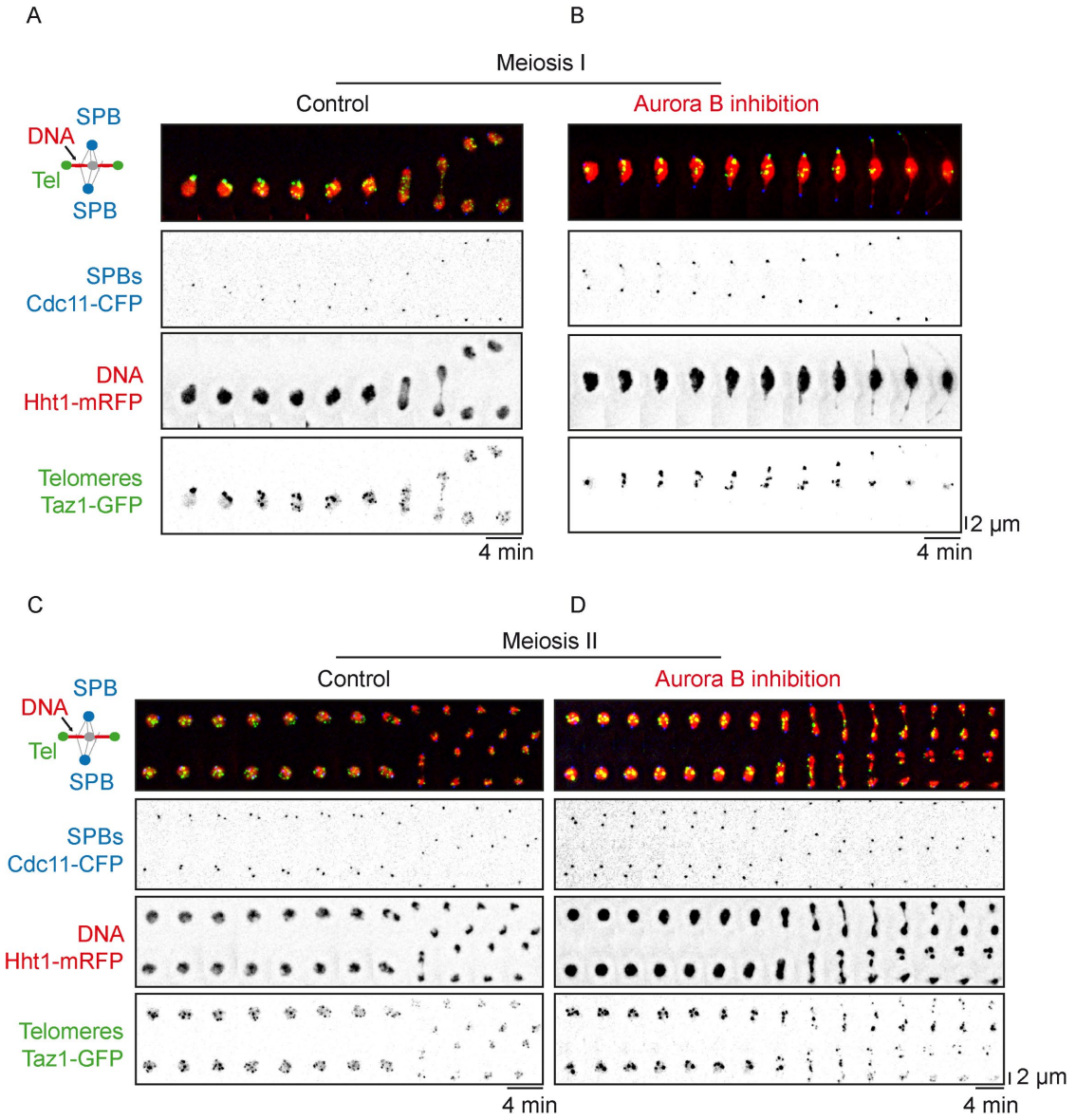

FIGURE 3: Aurora kinase is required for the separation of chromosome arms in meiosis I but not in meiosis II. Time-lapse imaging of chromosome arms disjunction in live meiotic *ark1-as3* cells. SPBs are visualized via Cdc11-CFP (blue), chromosome arms via Hht1-mRFP (histone H3, red), and telomeres via Taz1-GFP (green). Frames were acquired at intervals of 4 min. (A) Example of a cell during meiosis I progression. (B) Example of a cell during meiosis I progression in the presence of 10 µM 1-NA-PP1. (C) Example of a cell during meiosis II progression. (D) Example of a cell during meiosis II progression in the presence of 10 µM 1-NA-PP1.

telomere foci according to the distance between SPB foci. Data were measured from static images of *ark1-as3* cells ($n = 240$) under Aurora inhibition (red dots). Data from Figure 1C were reported as a control (black dots). (D) Selected frames from a movie of a live *ark1-as3* cell under meiosis II-specific Aurora inhibition. Telomeres are visualized via Taz1-GFP (green) and SPBs are visualized via Cdc11-CFP (red). Aurora inhibition was performed by adding 10 µM 1-NA-PP1, 10 min prior the start of image acquisition. (E) Telomere foci dynamics under meiosis II-specific Aurora inhibition. A kymograph and analysis of the movie shown in D is presented; the top and bottom meiosis II spindles of the movie are defined as spindle A and spindle B, respectively. The number of telomere foci is shown with a color code for each frame of the movie for both Spindle A (red box) and Spindle B (green box). After anaphase II onset, telomere foci number was counted separately in both segregated sets of chromosomes. (F) Number of telomeric foci under Aurora inhibition according to the distance between SPB foci. Data were measured on meiosis II movies of *ark1-as3* cells ($n = 10$) under meiosis II-specific Aurora inhibition (red dots). Aurora inhibition was performed by adding 10 µM 1-NA-PP1, 10 min prior the start of image acquisition. Data from Figure 1F was also reported as a control (black dots).

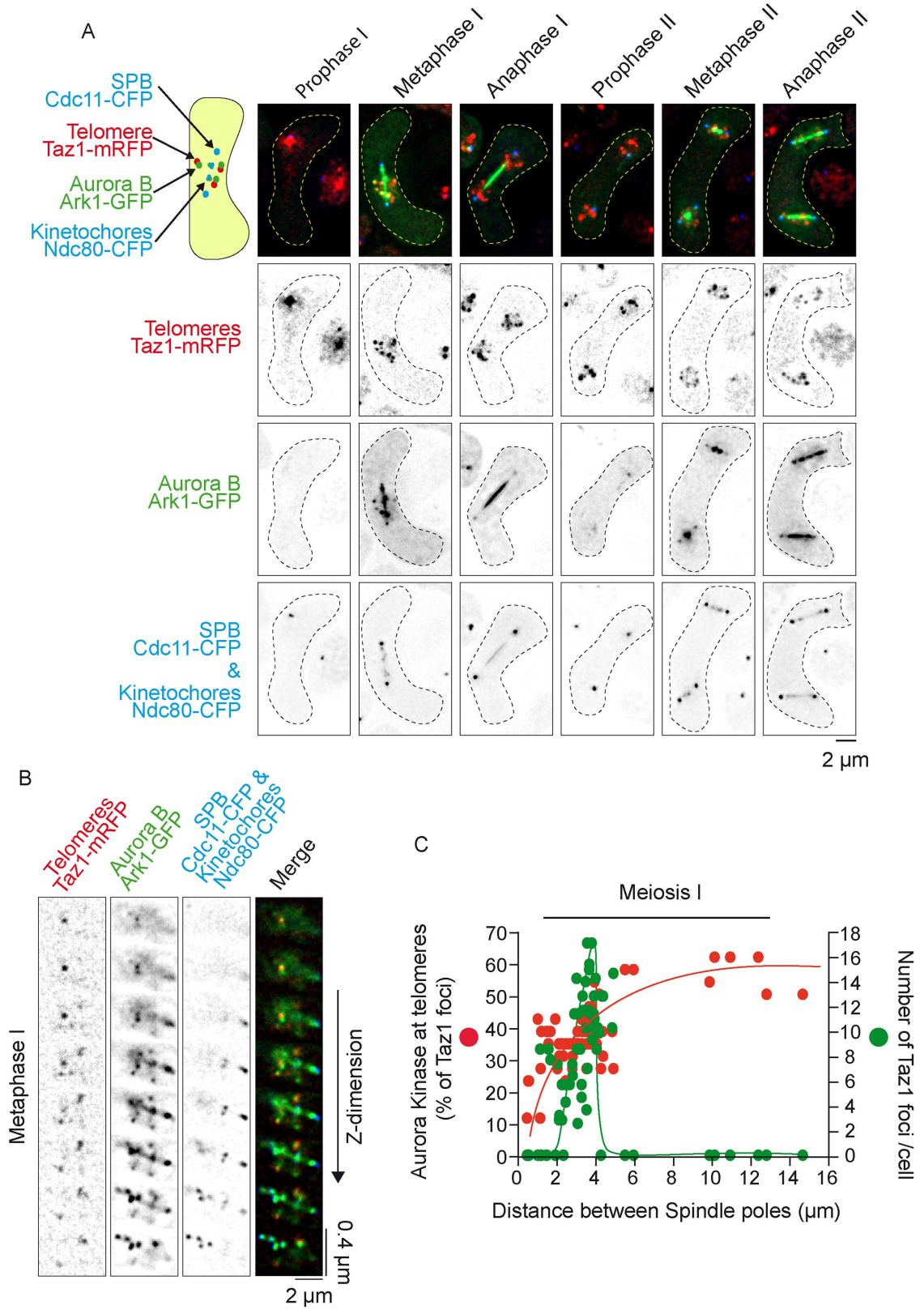

FIGURE 4: Aurora kinase localizes to telomeres during metaphase I but not during metaphase II. (A) Static images, representative of each meiotic phase, are shown. Telomeres are visualized via Taz1-mRFP (red), Aurora via Ark1-GFP (green), SPBs via Cdc11-CFP (blue), and KTs via Ndc80-CFP (blue). (B) Image of a metaphase I cell showing colocalization of Aurora B with telomeres. Telomeres are visualized via Taz1-mRFP (red), Aurora via Ark1-GFP (green), SPBs via Cdc11-CFP (blue), and KTs via Ndc80-CFP (blue). Each slice of a z-stack is shown along the vertical axis. (C) Dynamics of Aurora recruitment to telomeres during meiosis I. Both telomere foci number (Taz1-mRFP, red dots) and number of Aurora foci (Ark1-GFP, green dots) localized at telomeres were quantified on static images of cells undergoing meiosis I ($n = 67$).

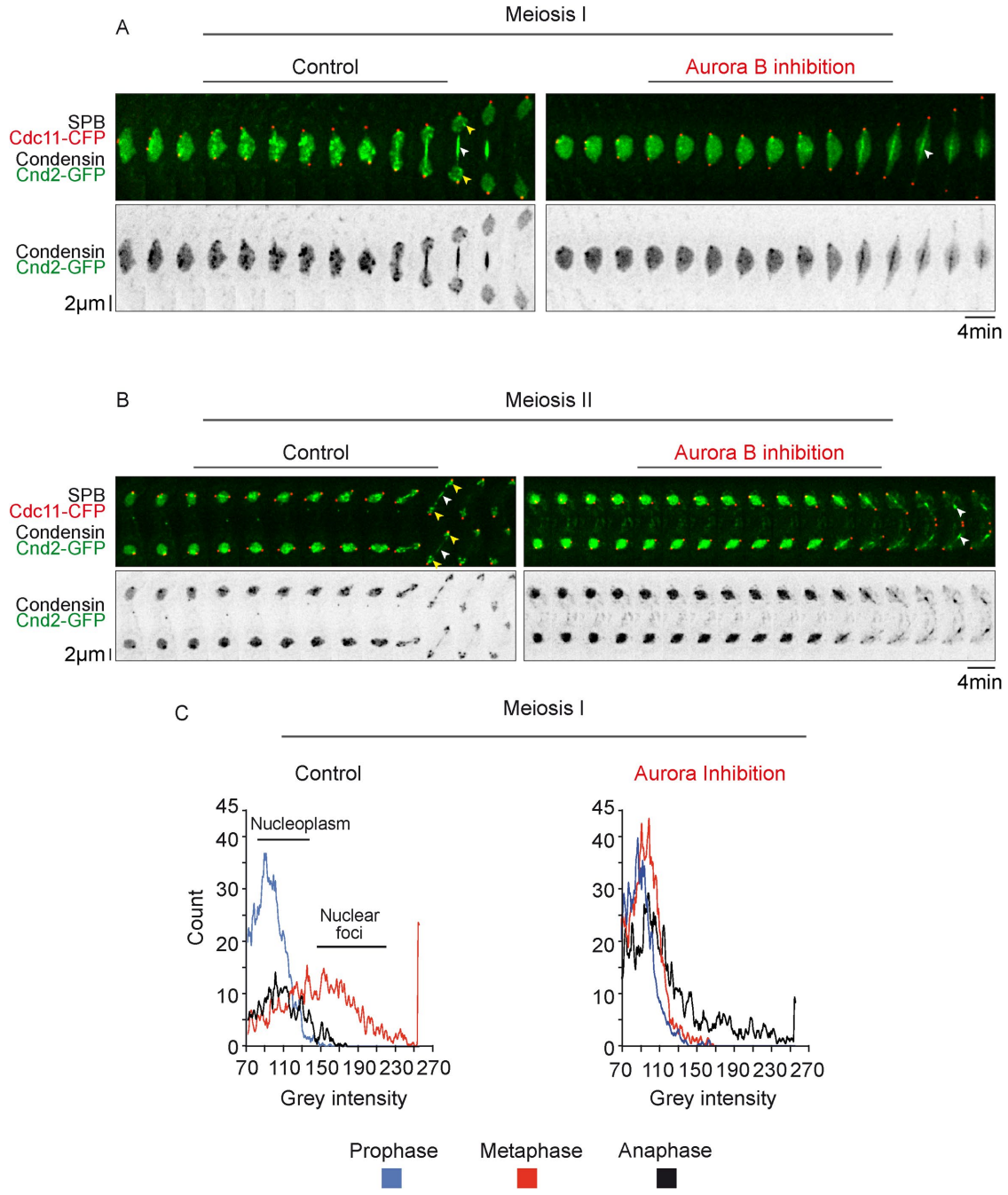

FIGURE 5: Aurora-dependent recruitment of condensin to chromosomes in both meiosis I and meiosis II. Condensin localization during meiotic progression is shown. SPBs are visualized via Cdc11-CFP (red) and condensin via Cnd2-GFP (green). White arrows show condensin localization to the spindle midzone in anaphase. Yellow arrows show chromosomal condensin during anaphase. (A) Frames from movies of *cnd2-GFP ark1-as3* cells undergoing meiosis I before (left panel) or after Aurora inhibition (right panel). (B) Frames from movies of *cnd2-GFP ark1-as3* cells undergoing meiosis II without (left panel) or with (right panel) Aurora inhibition. (C) Analysis of condensin recruitment using pixel intensity histograms.

on the meiotic cohesin Rec8, we added the 1-NA-PP1 inhibitor to *rec8Δ ark1-as3* cells expressing SPBs (Cdc11-cfp, red) and telomere (Taz1-gfp, green) markers and followed cells progressing into meiosis I (Figure 9, A and B). Strikingly, even in the absence of Rec8, Aurora inhibition significantly reduced the number of Taz1 foci, as opposed to untreated *rec8Δ* cells (Figure 9B). In agreement with this result, in *rec8*$^{+}$ cells, Rec8 remained solely associated in anaphase with the segregated centromeres (black arrows, Figure 9C) but no Rec8 foci colocalized with telomeres or chromosome arms following Aurora inhibition (Figure 9C, Aurora inhibition) as previously reported (Hauf *et al.*, 2007).

In contrast to the behavior of Rec8 in meiotic cells, the mitotic cohesin Rad21 is found predominantly at the leading edge of the nuclei undergoing prophase oscillations during meiosis I, just where the telomeres are clustered (Watanabe and Nurse, 1999; Yokobayashi *et al.*, 2003). In addition, it has been shown that the

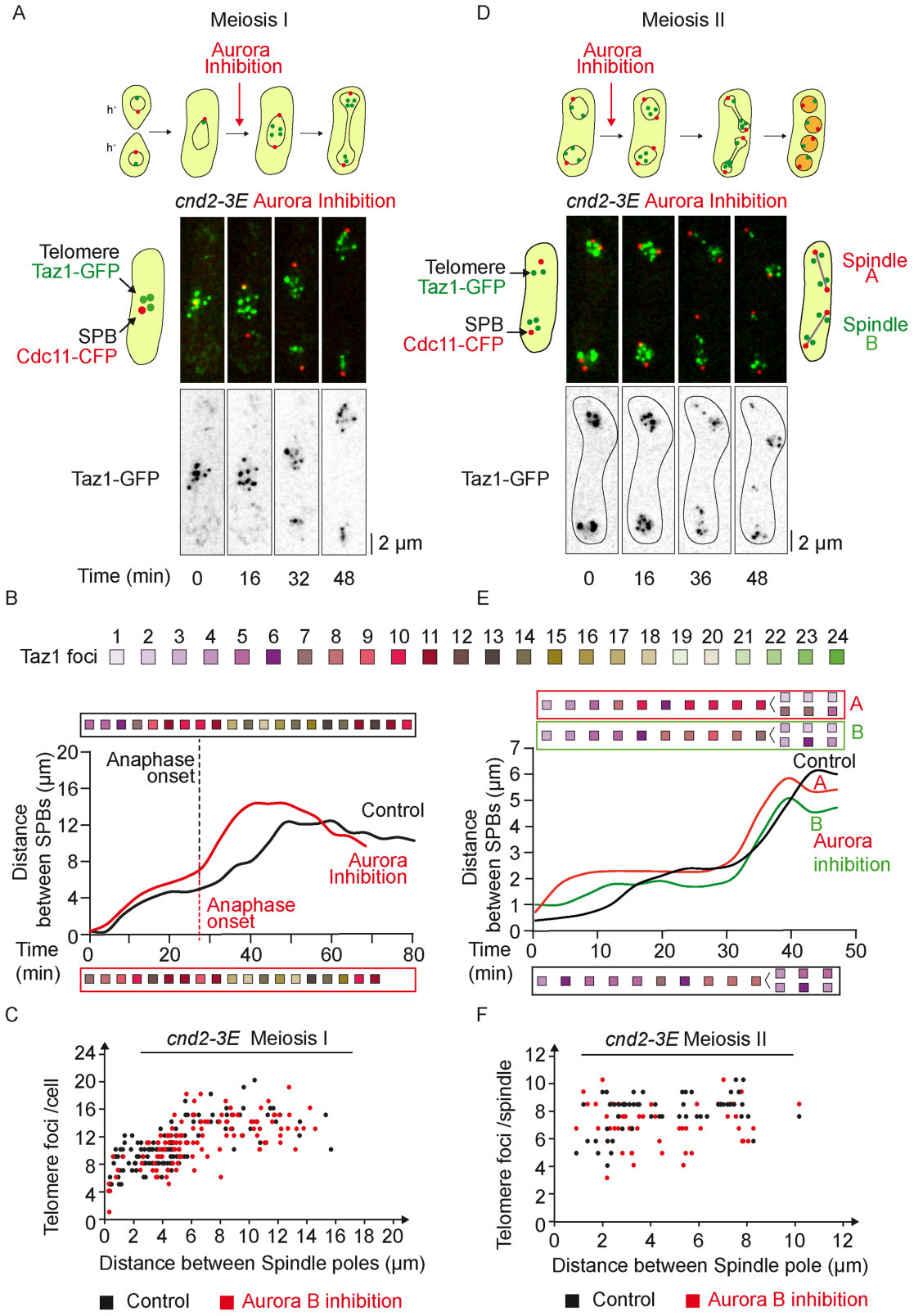

FIGURE 6: Condensin phosphomimetic mutant rescues telomere nondisjunction under Aurora inhibition in meiosis I. (A) Selected frames from a movie of a live *cnd2-3E ark1-as3* cell undergoing meiosis I under Aurora inhibition. Telomeres are visualized via Taz1-GFP (green) and SPBs via Cdc11-CFP (red). (B) Telomere foci dynamics during meiosis I in *cnd2-3E* cells. Analysis of the movie shown in A (Aurora Inhibition, red line and box), as well as the analysis of a control movie for *cnd2-3E* cell (Control, black line and box). The number of telomere foci is shown with a color code for each frame of the movie. (C) Number of telomere foci according to the distance between SPB foci in *cnd2-3E ark1-as3* cells undergoing meiosis I. Data were measured from static images in control (n = 137; black dots) and Aurora Inhibition

equational segregation of chromosomes in meiosis I in the absence of Rec8 depends on Rad21, which is then able to locate to the centromeres (Yokobayashi *et al.*, 2003). In light of these findings, we analyzed the localization of Rad21 in wild-type or Rec8-deleted cells (Supplemental Figure S5). In addition to the fraction colocalizing with the nucleolus/telomere region of prophase nuclei (Supplemental Figure S5A, control), we detected Rad21 foci at the telomere/nucleolar region of metaphase cells (Supplemental Figure S5A, control). These foci rapidly disappeared at the metaphase to anaphase transition as previously seen during mitosis (Reyes *et al.*, 2015). This pattern of Rad21 localization was also observed at the metaphase to anaphase transition when Rec8 was deleted (Supplemental Figure S5C, control), but as previously described, Rad21 also colocalized strongly to the centromere cluster in prophase of meiosis I (Supplemental Figure S5C, control). Interestingly, a small fraction of Rad21 remained at nucleoli and telomeres at anaphase when Aurora kinase was inactivated, in both control and *rec8Δ* cells (Supplemental Figure S5, A–D, aurora inhibition).

Together, these results demonstrate a role for Aurora at telomeres/chromosome arms in meiosis I, independently of the meiotic cohesin Rec8, and also suggest the existence of an Aurora- and condensin-independent mechanism to separate chromosome arms in meiosis I.

DISCUSSION

Our study reveals that the physical association of telomeres is tightly regulated during meiotic division. Interestingly, we observe both similarities and differences with mitosis in the dynamics of telomere separation. During mitosis, telomere foci first dissociate from the nuclear envelope (Fujita *et al.*, 2012) and then undergo separation in two discrete steps, both dependent on Aurora activity. Telomere dispersion occurs during metaphase, prior to chromosome segregation, while sister chromatid telomere disjunction is achieved during midanaphase (Reyes *et al.*, 2015). We previously proposed that the dissociation of the Shelterin complex in early mitosis initiates telomere dispersion, promotes condensin loading, and participates in chromosome arm separation. Similarly, in meiosis I, our study demonstrates that telomere separation occurs in two steps, dispersion in metaphase and disjunction during anaphase I. We further show that both steps are dependent on Aurora B kinase activity. Thus the mechanisms underlying telomere separation might be similar during mitosis and meiosis I (Figure 10).

In meiosis I, we show that Aurora B spatially targets distinct chromosomal domains (i.e., telomeres and centromeres) to control KT-MT attachment and telomere/chromosome arm separation. Previous studies have reported that the Shugoshin protein Sgo2 (Hauf *et al.*, 2007; Vanoosthuyse *et al.*, 2007) or the cohesin Rad21 (Morishita *et al.*, 2001) was required for the proper recruitment of Aurora at centromeres. However, what controls the loading of Aurora at fission yeast telomeres remains to be clarified since many factors seem to contribute to its localization. In mitosis, Aurora B promotes telomere and chromosome arm separation by phosphorylating and recruiting the condensin subunit Cnd2 to chromosomes (Nakazawa *et al.*, 2011; Tada *et al.*, 2011; Reyes *et al.*, 2015). Yet, the role of Aurora in correction of merotelic attachment is only partially dependent on the phosphorylation of Cnd2 condensin subunit since a phosphomimetic mutant of Cnd2 (*cnd2-3E*) only moderately bypasses chromosome arm separation defects following Aurora inhibition (Nakazawa *et al.*, 2011; Tada *et al.*, 2011; Reyes *et al.*, 2015).

In the present study, we went further in characterizing the role of condensin in KT-MT attachment and chromosome arm separation during meiosis. Through specific depletion of condensin in meiosis I, we demonstrate that faithful KT-MT attachment is largely independent of condensin. Instead, condensin plays an essential role in telomere/chromosome arm separation. A phosphomimetic mutant of *cnd2* (*cnd2-3E*) is able to bypass telomere/chromosome arm separation defects following Aurora inhibition. But again, in meiosis I, the function of Aurora in KT-MT attachment is completely independent of Cnd2 phosphorylation (Figure 10). How does condensin trigger chromosome arm-telomere separation? Similarly to the role of spindle elongation forces in anaphase error correction (Cimini *et al.*, 2004; Courtheoux *et al.*, 2009; Choi and McCollum, 2012; Gay *et al.*, 2012), we speculate that condensin may control telomere separation by mechanically pulling on chromosome arms.

During telophase of meiosis I, the spindle disassembles, telomeres reform clusters at the nuclear periphery prior to the onset of meiosis II. Thus, the reclustering of telomeres at the nuclear periphery is independent of de novo DNA replication. Finally, in meiosis II, telomeres separate in a single step during metaphase prior to chromosome segregation and independently of Aurora activity. In this respect, the dynamics of telomere separation in meiosis II differ from meiosis I and mitosis. In meiosis II, Aurora B only localizes to centromeres, which allowed us to separate the functions of the CPC at those chromosomal loci. Our observation that condensin is largely dispensable in meiosis II for telomere/chromosome arm separation might reflect lower opposing forces to spindle elongation in meiosis II as opposed to mitosis or meiosis I. However, we found no clear differences in the rate of spindle elongation in mitosis/meiosis I or meiosis II cells arguing against this hypothesis. Alternatively, a chromatin compaction mechanism associated with spore formation might compensate for reduced condensin activity during meiosis II.

A major difference between meiosis I and II is the specific presence in meiosis II of a phenomenon called "virtual" NEBD (Arai *et al.*, 2010; Asakawa *et al.*, 2010), a key event for *S. pombe* meiosis (Asakawa *et al.*, 2016; Flor-Parra *et al.*, 2018). Although the nuclear envelope and the Nuclear Pore Complexes remain assembled throughout the entire meiotic division, nuclear proteins are able to diffuse transiently into the cytoplasm at the onset of anaphase B of meiosis II. Consequently, nuclear and cytoplasmic molecules appear to be mixed in a process resembling an open mitosis. This

(*n* = 121; red dots). (D) Selected frames from a movie of a live *cnd2-3E ark1-as3* cell under meiosis II-specific Aurora inhibition. Telomeres are visualized via Taz1-GFP and SPBs via Cdc11-CFP (red). (E) Telomere foci dynamics in *cnd2-3E ark1-as3* cells under meiosis II-specific Aurora inhibition. Analysis of the movie shown in D; the top and bottom meiosis II spindles of the movie are defined as spindle A and spindle B, respectively. The number of telomere foci is shown with a color code for each frame of the movie for both Spindle A (red box) and Spindle B (green box). Analysis of a control *cnd-3E ark1-as3* cell in meiosis II (Control, black line and box). After anaphase II onset, the number of telomere foci was counted separately in both sets of segregated chromosomes. (F) Number of telomere foci according to the distance between SPB foci during meiosis II in *cnd2-3E ark1-as3* cells. Data were measured in meiosis II in control (*n* = 6 movies; black dots) and after Aurora inhibition (*n* = 8 movies; red dots).

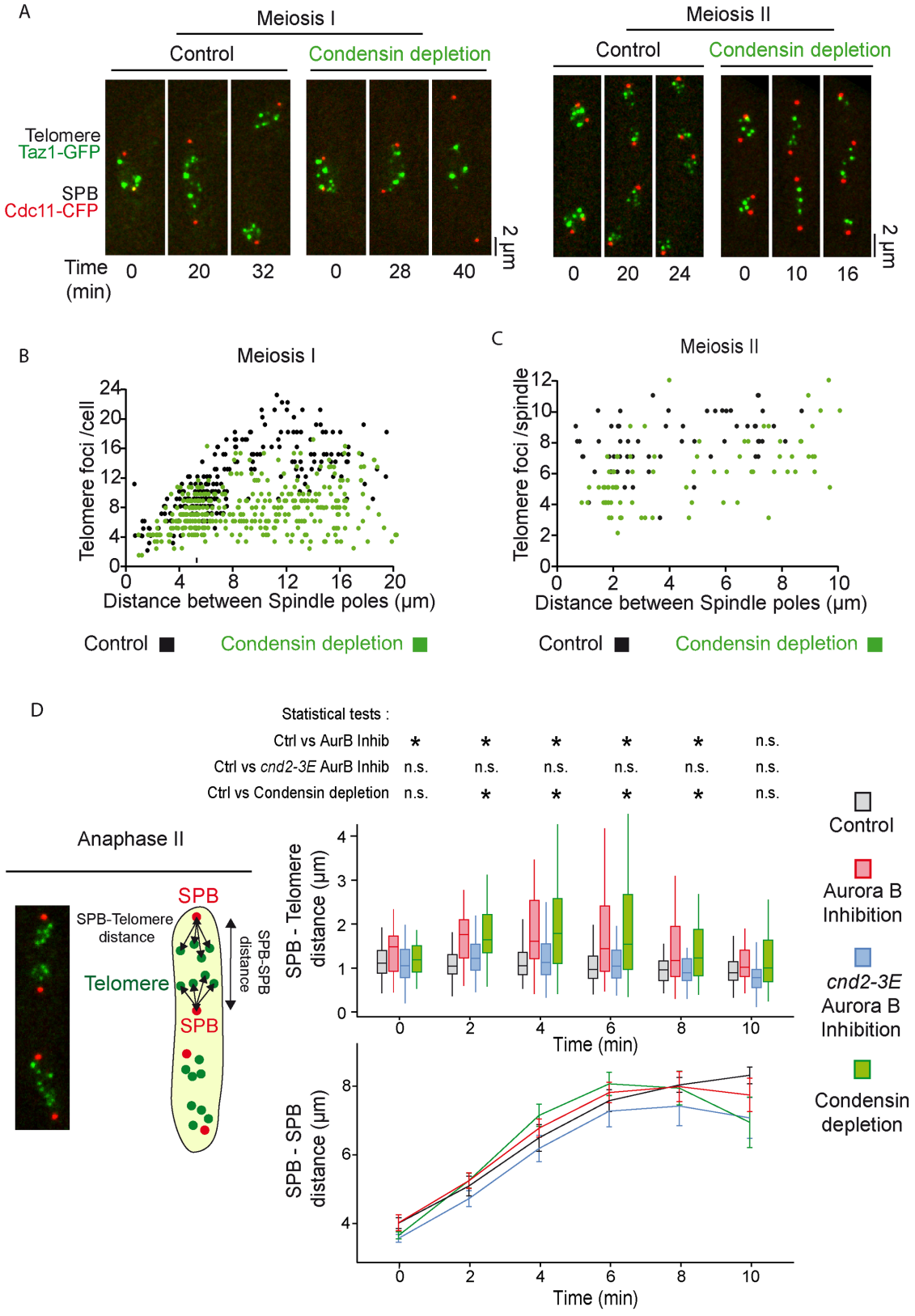

FIGURE 7: Telomere separation is achieved in meiosis II despite condensin depletion. (A) Selected frames from movies of *cut14-shutoff* cells undergoing meiosis I (left panel) and meiosis II (right panel). Telomeres are visualized via Taz1-GFP (green) and SPBs are visualized via Cdc11-CFP (red). Condensin depletion is induced by the addition of 0.5 mM of Auxin and 5 µg/ml of thiamine. Image acquisition was started after 3 h of induction for meiosis I and after 2 h 20 min for meiosis II. (B) Number of telomere foci according to the distance between SPB foci in meiosis I. Condensin depletion (green dots) is induced by the addition of 0.5 mM of Auxin and 5 µg/ml of thiamine. Control (black dots) corresponds to images of *cut14-so* cells grown in the absence of Auxin and thiamine. Data were measured from static images of control

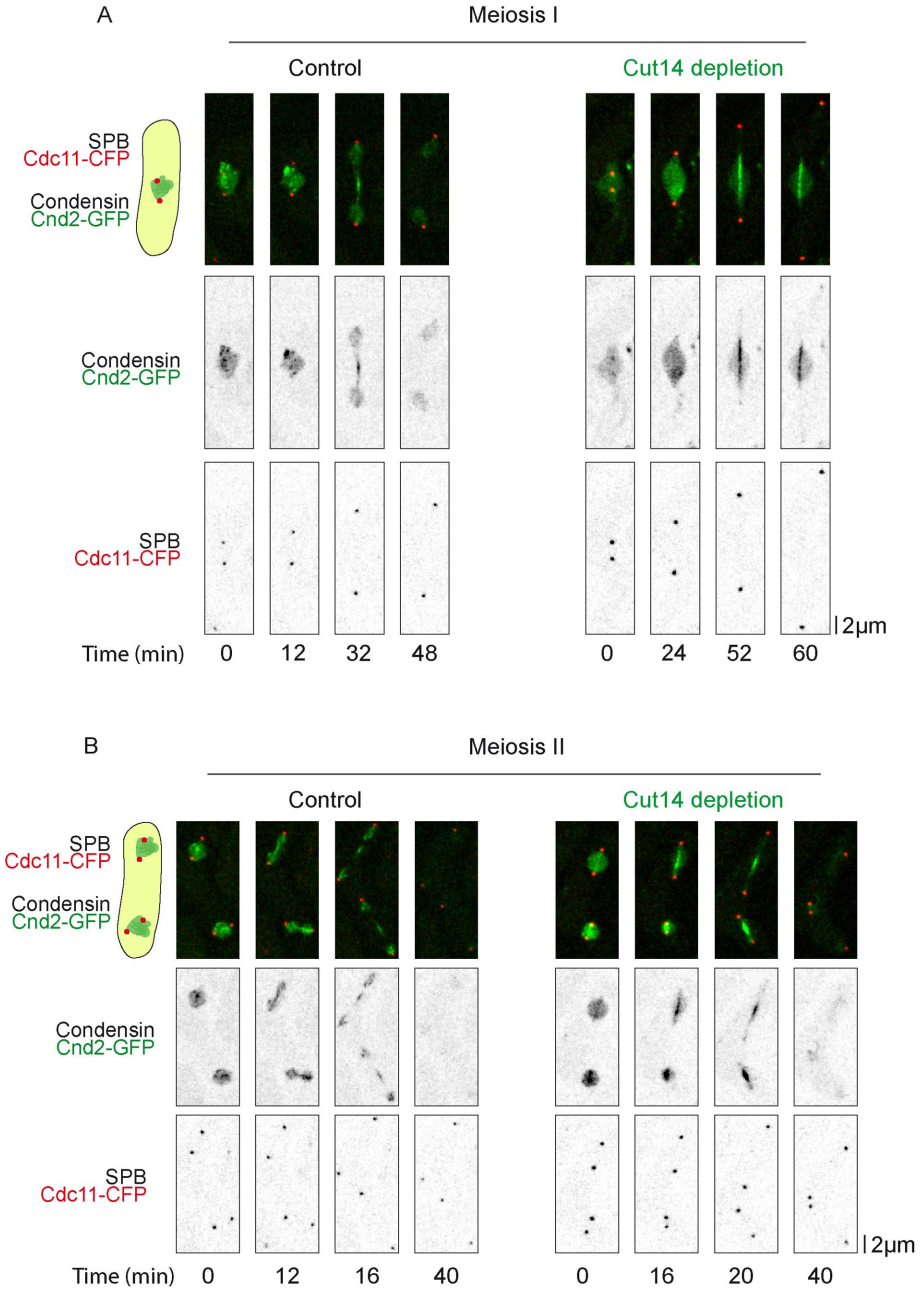

FIGURE 8: Cut14 depletion induces a loss of condensin localization to chromosomes. Selected frames from movies showing condensin localization upon Cut14 depletion in meiosis I (A) and meiosis II (B). SPBs are visualized via Cdc11-CFP (red) and condensin is visualized via Cnd2-GFP (green). WT (Control) and *cut14-so* (Cut14 depletion) cells were exposed to 0.5 mM of Auxin and 5 μg/ml of thiamine for 3 h in A and 2 h 20 min in B.

phenomenon certainly accounts for some of our observations such as the disappearance of condensin signal from the nucleus following Aurora inhibition in meiosis II. Hence, it remains possible that the diffusion of several nuclear proteins in meiosis II participates in this noncanonical chromosome segregation event. A second difference between meiosis I or II is the presence of the forespore membrane in meiosis II, which encapsulates the nucleus and produces forces for cell division (Akera *et al.*, 2012). Markedly, it has been shown that interpolar MTs were dispensable in meiosis II for spindle pole separation (Akera *et al.*, 2012). Finally, it is formally possible that the lack of DNA replication prior to meiosis II might change the requirement for condensin activity during the subsequent division. New cohesion on chromosome arms cannot be generated between meiosis I and II in the absence of de novo DNA replication (Uhlmann and Nasmyth, 1998; Toth *et al.*, 1999; Watanabe *et al.*, 2001). Meiosis II chromosomes may thus lack some specific features dependent on cohesins. In mitosis, the dispersal of Rad21 from telomeres relies upon Aurora B (Reyes *et al.*, 2015). It has also been reported that cohesin participates in subtelomeric heterochromatin maintenance in fission yeast probably by acting locally on Swi6/HP1 binding in the subtelomeric region (Dheur *et al.*, 2011). However, we found that the role of Aurora B on telomere/chromosome arm separation in meiosis I was independent of the key meiotic cohesin, Rec8. In addition, Rec8 was not enriched at telomeres before or after Aurora inhibition. Rec8 was first identified in a genetic screen for mutants showing a decrease in recombination at the ade6 locus (Ponticelli and Smith, 1989) and several features of meiotic chromosomes were shown to be disrupted in *rec8Δ* cells, including the formation of chiasmata (Molnar *et al.*, 1995; Watanabe and Nurse, 1999; Ellermeier and Smith, 2005). Our results therefore suggest that the telomere dissociation pathway in meiosis I operates independently of chiasma resolution.

cells ($n = 226$; black dots) and cells submitted to condensin depletion for 3 h ($n = 337$; green dots). (C) Number of telomere foci according to the distance between SPB foci in meiosis II. Condensin depletion (green dots) is induced by the addition of 0.5 mM of Auxin and 5 μg/ml of thiamine. Control (black dots) corresponds to *cut14-so* cells filmed in the absence of Auxin and thiamine. Data were measured on movies ($n = 8$ spindles, control cells, black dots; $n = 8$ spindles of cells depleted for condensin, green dots). (D) Dynamics of telomere separation in meiosis II. Movies of cells in meiosis II were used to calculate the distances between each telomere foci and its nearest SPB focus ($n = 8$ spindles for each condition). Top graph: the telomere to SPB distance is plotted according to the time from anaphase II onset which corresponds to $t = 0$. The average corresponding SPB to SPB distance for the same movies is reported in the bottom graph (mean ± SD for each condition). Control (black boxes and line) are *ark1-as3* cells filmed in the absence of 1-NA-PP1; Aurora inhibition (red boxes and red line) is performed on *ark1-as3* cells, *cnd2-3E ark1-as3* cells (blue boxes and blue line) treated with 10 μM 1-NA-PP1; Cut14 depletion (green boxes and green line) is performed on *cut14-so* cells by the addition of 0.5 mM of Auxin and 5 μg/ml of thiamine. *$p < 0.01$ Mann–Whitney nonparametric test.

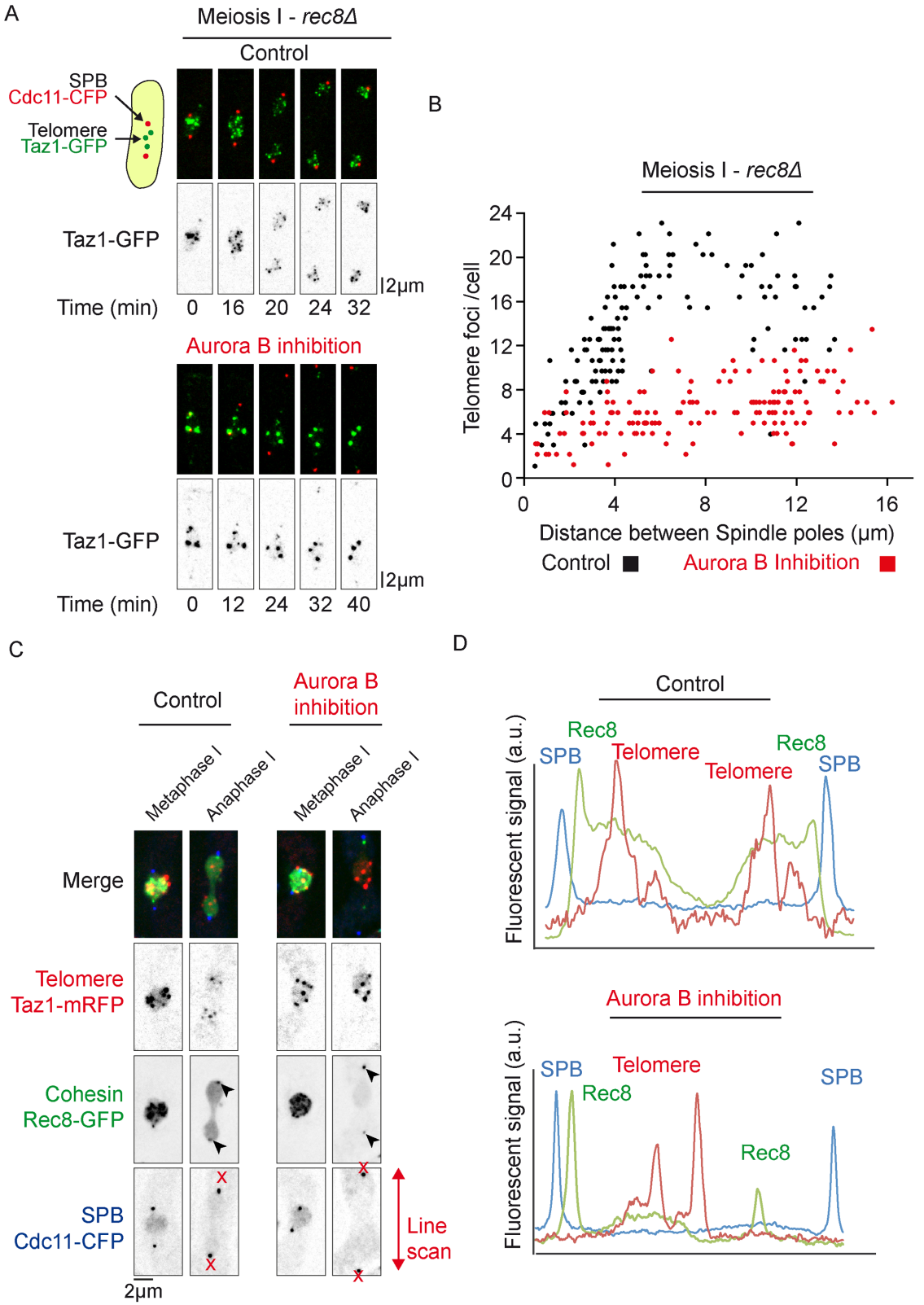

FIGURE 9: Aurora kinase is required for telomere separation in meiosis I independently of the meiotic cohesin Rec8. (A) Selected frames from a movie of *rec8Δ ark1-as3* cell undergoing meiosis I. Telomeres are visualized via Taz1-GFP (green) and SPBs are visualized via Cdc11-CFP (red). (B) Number of telomere foci according to the distance between SPB foci in *rec8Δ ark1-as3* cells undergoing meiosis I. Data were measured from static images of *rec8Δ ark1-as3* cells ($n = 142$, black dots) and *rec8Δ ark1-as3* cells under Aurora Inhibition ($n = 148$, red dots). (C) Meiotic cohesin Rec8 localization during meiosis I. Static images of live cells representative of metaphase I and anaphase I. Telomeres are visualized via Taz1-mRFP (red), meiotic cohesin via Rec8-GFP (green), and SPBs via Cdc11-CFP (blue). Black arrows show Rec8 retained at centromeres during anaphase I. (D) Line scans analysis of the cells shown in C, for control (top panel) and Aurora inhibition (bottom panel).

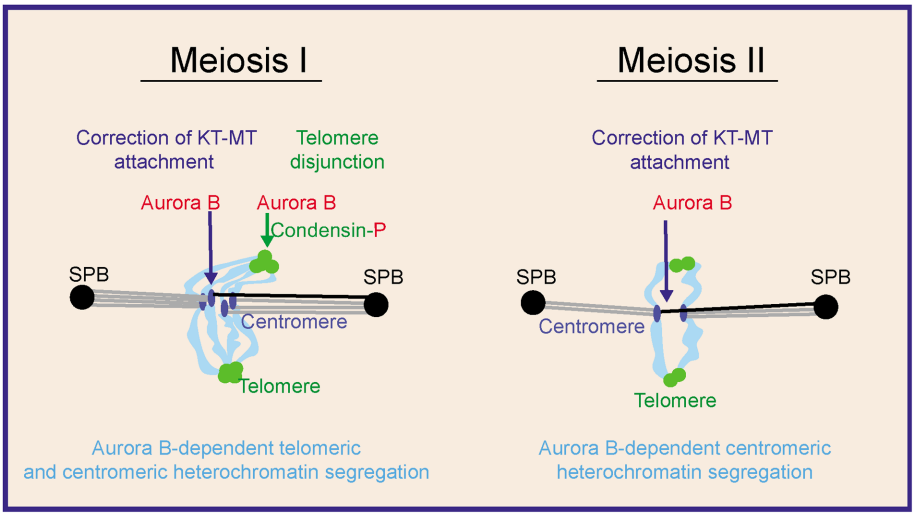

FIGURE 10: Model summarizing the respective roles of Aurora and condensin in centromeric, telomeric or chromosome arms segregation in meiosis I and II. Schematic representation illustrating the regulation of telomere, chromosome arms, and centromere dissociation throughout meiosis.

Conversely and similarly to our observations in mitosis, we were able to detect a subfraction of Rad21 cohesin that remained associated with telomeres/nucleolus following Aurora inhibition. Since it has been shown that only 5% cleavage of Rad21 protein is sufficient to segregate chromosomes (Tomonaga *et al.*, 2000), we cannot exclude that this subfraction of Rad21 during anaphase is also sufficient to maintain telomere entanglements in meiosis I. If this is the case, the role of Aurora kinase at fission yeast telomeres resembles the function of tankyrase 1, since the resolution of sister chromatid cohesion between telomeres in human cells also occurs in early mitosis but has a specific requirement for the poly(ADP-ribose) polymerase tankyrase 1 (Dynek and Smith, 2004; Bisht *et al.*, 2013).

In conclusion, it is often mentioned in the scientific literature that chromosome segregation in mitosis or meiosis II requires similar mechanisms since both processes involve the separation of sister chromatids to the two daughter cells. Our study challenges this view by revealing critical differences existing between mitosis and meiosis II in the control of chromosome segregation. Unlike mitosis or even meiosis I, chromosome segregation during meiosis II is largely independent of Aurora kinase and condensin, arguing that it most likely involves hitherto ignored noncanonical mechanisms.

MATERIALS AND METHODS

S. pombe strains and culture

Media, growth, maintenance of strains, and genetic methods were as described (Moreno *et al.*, 1991). All strains used in this study are listed in Supplemental Table S1. All featured alleles are created from original strains, referenced and described in Supplemental Table S1. Crosses for strain generation were performed by tetrad dissection and selected through drug resistance, prototrophy for specific amino acids, or visual selection for fluorescent markers. The *cnd2-3E* allele was selected in *ark1-as3* strains by testing the resistance to Aurora inhibition with 1 µM 1-NA-PP1. Strains were grown on YES solid media at 25°C. Strains carrying Cut14 under the expression of the nmt81 promoter were grown on EMM+N solid media at 25°C. To induce meiosis, h+ and h– strains were mixed (or h90 alone) and spread on EMM-N solid media at 25°C overnight.

Live-cell microscopy

To increase the density of meiotic cells prior condensin-independent mechanism of chromosome segregation in meiosis condensin-independent mechanism of chromosome segregation in meiosis to filming, crosses were suspended in liquid EMM media and aggregates of meiotic cells were left to sediment at the bottom of the tube. Supernatant was discarded and cells were resuspended three times. Meiotic cells were spread on a plug of EMM filled with 2% agarose in an imaging chamber (CoverWell imaging chamber 22 mm × 1.7 mm; Grace Bio-Labs). The imaging chamber was sealed with a 22 × 22 glass coverslip.

Images were acquired with a CCD CoolSNAP HQ2 camera (Roper Scientific) fitted to a DM6000 upright microscope (Leica) with a ×100 1.40 NA objective or a CCD Retiga R6 camera (QImaging) fitted to a DM6B upright microscope with a ×100 1.44 NA objective using Metamorph as a software. Z-stacks of 9 planes spaced by 0.7 µm were typically acquired at 4-min intervals (2 min for anaphase II analysis in Figure 7D) for the entire duration of meiosis I and II at 25°C.

For CENII segregation analysis in Supplemental Figure S2 and Supplemental Figure S4 as well as for spindle elongation measurements in Supplemental Figure S1A, images were acquired with a Neo sCMOS camera (Andor) fitted to an Eclipse Ti inverted microscope (Nikon) with a ×60 1.40 NA objective using MicroManager as a software at 2-min intervals for 1 h at 25°C.

Aurora kinase inhibition and condensin depletion

The *ark1-as3* analog-sensitive allele (Koch *et al.*, 2011) was used to perform Ark1 inhibition. To inhibit Aurora in meiosis I or II, the imaging media was supplemented with 10 µM 1-NA-PP1 (Euromedex). However, to specifically inhibit Aurora kinase in meiosis II, image acquisition started exactly 10 min after the spreading of cells on the imaging media containing 1-NA-PP1, and only cells starting meiosis II were filmed. This protocol allows imaging of cells that underwent normal chromosome segregation in meiosis I.

Condensin depletion was performed using the *cut14-so* strain previously described (Kakui *et al.*, 2017) that combines transcriptional repression of *cut14* under the nmt81 thiamine-repressible promoter and Cut14 depletion using an Auxin-Inducible Degron (AID) system. To induce condensin depletion, the imaging media was supplemented with 0.5 mM of 1-Naphthaleneacetic acid (Sigma) and 5 µg/ml of thiamine. For condensin depletion in meiosis I, image acquisition was started 3 h after spreading the cells on the imaging media containing Naphthaleneacetic acid. For condensin depletion in meiosis II, image acquisition was started between 2 h and 2 h 30 min after spreading cells on the imaging media containing Naphthaleneacetic acid since longer induction caused meiosis I spindle collapse during the incubation period.

Image processing and analysis

All image processing and analysis was performed using ImageJ. Deconvolution of Z-stacks and PSF generation were performed using the DeconvolutionLab and PSF Generator ImageJ plugins. Deconvolved stacks were combined using maximum intensity Z-projections. If needed, sample drifting over time was corrected with the

MultiStackReg ImageJ plugin. Figures were assembled with the R ggplot2 package, ImageJ, Microsoft Excel, and Adobe Illustrator. The number of telomere and Ark1 foci was assessed manually. Distances shown in Supplemental Figure S1C were measured on non-projected Z-planes. We measured the distances between the center of the telomere focus to the center of the nuclear envelope fluorescent signal. Distances in other figures were measured on Z-projections between the centers of telomere to SPB foci. In Supplemental Figure S2 and Supplemental Figure S4, lagging centromeres were defined as CENII foci that don't colocalize with an SPB during anaphase I or II. Unequal centromere segregation was defined as a single CENII signal observed on a single SPB during anaphase I or II. In meiosis II, the two spindles were considered independently of one another. Spindle elongation profiles shown in Supplemental Figure S1A were measured on the movies of CENII segregation analysis. Anaphase onset was manually annotated and defined as the sharp increase in spindle elongation speed and spindle elongation curves were all aligned at anaphase onset.

For the analysis of condensin particle size, we performed an histogram of pixel intensities using imageJ.

Statistical analysis

Statistical tests were performed using R. Sample sizes and p values are reported in Supplemental Table S2. Groups were compared in Figure 7D and Supplemental Figure S1C using Mann–Whitney non-parametric tests with $p < 0.01$ considered significant. Phenotype frequencies between conditions in Supplemental Figure S2 and Supplemental Figure S4 were compared using Chi-square tests; contingency tables are presented in Supplemental Table S2.

ACKNOWLEDGMENTS

We thank J. Cooper, J.P. Javerzat, and M. Yanagida for supplying strains; S. Hauf for supplying the *ark1-as3* mutant and Y. Watanabe for the *cnd2-3E* mutant; and J.P. Javerzat and Dean Dawson for helpful discussions. J.B. was supported by University MRT and Fondation pour la Recherche Medicale (FRM) fellowships number, FDT201904008123. This work was funded by the ANR-16-CE12-0015 -TeloMito-2016 and l'Association de la Recherche sur le Cancer (ARC), fonctionnement, 2016. The microscopy equipment was funded by the CNRS and ARC.

REFERENCES

Akera T, Sato M, Yamamoto M (2012). Interpolar microtubules are dispensable in fission yeast meiosis II. Nat Commun 3, 695.

Arai K, Sato M, Tanaka K, Yamamoto M (2010). Nuclear compartmentalization is abolished during fission yeast meiosis. Curr Biol 20, 1913–1918.

Asakawa H, Kojidani T, Mori C, Osakada H, Sato M, Ding DQ, Hiraoka Y, Haraguchi T (2010). Virtual breakdown of the nuclear envelope in fission yeast meiosis. Curr Biol 20, 1919–1925.

Asakawa H, Yang HJ, Hiraoka Y, Haraguchi T (2016). Virtual nuclear envelope breakdown and its regulators in fission yeast meiosis. Front Cell Dev Biol 4, 5.

Bisht KK, Daniloski Z, Smith S (2013). SA1 binds directly to DNA through its unique AT-hook to promote sister chromatid cohesion at telomeres. J Cell Sci 126, 3493–3503.

Carmena M, Wheelock M, Funabiki H, Earnshaw WC (2012). The chromosomal passenger complex (CPC): from easy rider to the godfather of mitosis. Nat Rev Mol Cell Biol 13, 789–803.

Chan CS, Botstein D (1993). Isolation and characterization of chromosome-gain and increase-in-ploidy mutants in yeast. Genetics 135, 677–691.

Chan FL, Vinod B, Novy K, Schittenhelm RB, Huang C, Udugama M, Nunez-Iglesias J, Lin JI, Hii L, Chan J, Pickett HA, Daly RJ, Wong LH (2017). Aurora Kinase B, a novel regulator of TERF1 binding and telomeric integrity. Nucleic Acids Res 45, 12340–12353.

Chikashige Y, Ding DQ, Funabiki H, Haraguchi T, Mashiko S, Yanagida M, Hiraoka Y (1994). Telomere-led premeiotic chromosome movement in fission yeast. Science 264, 270–273.

Chikashige Y, Hiraoka Y (2001). Telomere binding of the Rap1 protein is required for meiosis in fission yeast. Curr Biol 11, 1618–1623.

Chikashige Y, Tsutsumi C, Yamane M, Okamasa K, Haraguchi T, Hiraoka Y (2006). Meiotic proteins bqt1 and bqt2 tether telomeres to form the bouquet arrangement of chromosomes. Cell 125, 59–69.

Choi SH, McCollum D (2012). A role for metaphase spindle elongation forces in correction of merotelic kinetochore attachments. Curr Biol 22, 225–230.

Cimini D, Cameron LA, Salmon ED (2004). Anaphase spindle mechanics prevent mis-segregation of merotelically oriented chromosomes. Curr Biol 14, 2149–2155.

Cimini D, Wan X, Hirel CB, Salmon ED (2006). Aurora kinase promotes turnover of kinetochore microtubules to reduce chromosome segregation errors. Curr Biol 16, 1711–1718.

Cleveland DW, Mao Y, Sullivan KF (2003). Centromeres and kinetochores: from epigenetics to mitotic checkpoint signaling. Cell 112, 407–421.

Cooper JP, Nimmo ER, Allshire RC, Cech TR (1997). Regulation of telomere length and function by a Myb-domain protein in fission yeast. Nature 385, 744–747.

Cooper JP, Watanabe Y, Nurse P (1998). Fission yeast Taz1 protein is required for meiotic telomere clustering and recombination. Nature 392, 828–831.

Courtheoux T, Gay G, Gachet Y, Tournier S (2009). Ase1/Prc1-dependent spindle elongation corrects merotely during anaphase in fission yeast. J Cell Biol 187, 399–412.

Dheur S, Saupe SJ, Genier S, Vazquez S, Javerzat JP (2011). Role for cohesin in the formation of a heterochromatic domain at fission yeast subtelomeres. Mol Cell Biol 31, 1088–1097.

Dynek JN, Smith S (2004). Resolution of sister telomere association is required for progression through mitosis. Science 304, 97–100.

Ellermeier C, Smith GR (2005). Cohesins are required for meiotic DNA breakage and recombination in Schizosaccharomyces pombe. Proc Natl Acad Sci USA 102, 10952–10957.

Flor-Parra I, Iglesias-Romero AB, Salas-Pino S, Lucena R, Jimenez J, Daga RR (2018). Importin alpha and vNEBD Control Meiotic Spindle Disassembly in Fission Yeast. Cell Reports 23, 933–941.

Fujita I, Nishihara Y, Tanaka M, Tsujii H, Chikashige Y, Watanabe Y, Saito M, Ishikawa F, Hiraoka Y, Kanoh J (2012). Telomere-nuclear envelope dissociation promoted by Rap1 phosphorylation ensures faithful chromosome segregation. Curr Biol 22, 1932–1937.

Gay G, Courtheoux T, Reyes C, Tournier S, Gachet Y (2012). A stochastic model of kinetochore-microtubule attachment accurately describes fission yeast chromosome segregation. J Cell Biol 196, 757–774.

Giet R, Glover DM (2001). Drosophila aurora B kinase is required for histone H3 phosphorylation and condensin recruitment during chromosome condensation and to organize the central spindle during cytokinesis. J Cell Biol 152, 669–682.

Gregan J, Polakova S, Zhang L, Tolic-Norrelykke IM, Cimini D (2011). Merotelic kinetochore attachment: causes and effects. Trends Cell Biol 21, 374–381.

Gregan J, Riedel CG, Pidoux AL, Katou Y, Rumpf C, Schleiffer A, Kearsey SE, Shirahige K, Allshire RC, Nasmyth K (2007). The kinetochore proteins Pcs1 and Mde4 and heterochromatin are required to prevent merotelic orientation. Curr Biol 17, 1190–1200.

Hauf S, Biswas A, Langegger M, Kawashima SA, Tsukahara T, Watanabe Y (2007). Aurora controls sister kinetochore mono-orientation and homolog bi-orientation in meiosis-I. EMBO J 26, 4475–4486.

Hayashi MT, Cesare AJ, Fitzpatrick JA, Lazzerini-Denchi E, Karlseder J (2012). A telomere-dependent DNA damage checkpoint induced by prolonged mitotic arrest. Nat Struct Mol Biol 19, 387–394.

Hiraoka Y, Dernburg AF (2009). The SUN rises on meiotic chromosome dynamics. Dev Cell 17, 598–605.

Kakui Y, Rabinowitz A, Barry DJ, Uhlmann F (2017). Condensin-mediated remodeling of the mitotic chromatin landscape in fission yeast. Nat Genet 49, 1553–1557.

Kelly AE, Funabiki H (2009). Correcting aberrant kinetochore microtubule attachments: an Aurora B-centric view. Curr Opin Cell Biol 21, 51–58.

Klutstein M, Fennell A, Fernandez-Alvarez A, Cooper JP (2015). The telomere bouquet regulates meiotic centromere assembly. Nat Cell Biol 17, 458–469.

Koch A, Krug K, Pengelley S, Macek B, Hauf S (2011). Mitotic substrates of the kinase aurora with roles in chromatin regulation identified through quantitative phosphoproteomics of fission yeast. Sci Signal 4, rs6.

Kotwaliwale CV, Frei SB, Stern BM, Biggins S (2007). A pathway containing the Ipl1/aurora protein kinase and the spindle midzone protein Ase1 regulates yeast spindle assembly. Dev Cell 13, 433–445.

Lampson MA, Cheeseman IM (2011). Sensing centromere tension: Aurora B and the regulation of kinetochore function. Trends Cell Biol 21, 133–140.
Leverson JD, Huang HK, Forsburg SL, Hunter T (2002). The Schizosaccharomyces pombe aurora-related kinase Ark1 interacts with the inner centromere protein Pic1 and mediates chromosome segregation and cytokinesis. Mol Biol Cell 13, 1132–1143.
Lipp JJ, Hirota T, Poser I, Peters JM (2007). Aurora B controls the association of condensin I but not condensin II with mitotic chromosomes. J Cell Sci 120, 1245–1255.
Meyer RE, Kim S, Obeso D, Straight PD, Winey M, Dawson DS (2013). Mps1 and Ipl1/Aurora B act sequentially to correctly orient chromosomes on the meiotic spindle of budding yeast. Science 339, 1071–1074.
Moiseeva V, Amelina H, Collopy LC, Armstrong CA, Pearson SR, Tomita K (2017). The telomere bouquet facilitates meiotic prophase progression and exit in fission yeast. Cell discovery 3, 17041.
Molnar M, Bahler J, Sipiczki M, Kohli J (1995). The rec8 gene of Schizosaccharomyces pombe is involved in linear element formation, chromosome pairing and sister-chromatid cohesion during meiosis. Genetics 141, 61–73.
Mora-Bermudez F, Gerlich D, Ellenberg J (2007). Maximal chromosome compaction occurs by axial shortening in anaphase and depends on Aurora kinase. Nat Cell Biol 9, 822–831.
Moreno S, Klar A, Nurse P (1991). Molecular genetic analysis of fission yeast Schizosaccharomyces pombe. Methods Enzymol 194, 795–823.
Morishita J, Matsusaka T, Goshima G, Nakamura T, Tatebe H, Yanagida M (2001). Bir1/Cut17 moving from chromosome to spindle upon the loss of cohesion is required for condensation, spindle elongation and repair. Genes Cells 6, 743–763.
Nakazawa N, Mehrotra R, Ebe M, Yanagida M (2011). Condensin phosphorylated by the Aurora-B-like kinase Ark1 is continuously required until telophase in a mode distinct from Top2. J Cell Sci 124, 1795–1807.
Nakazawa N, Nakamura T, Kokubu A, Ebe M, Nagao K, Yanagida M (2008). Dissection of the essential steps for condensin accumulation at kinetochores and rDNAs during fission yeast mitosis. J Cell Biol 180, 1115–1131.
Ono T, Fang Y, Spector DL, Hirano T (2004). Spatial and temporal regulation of Condensins I and II in mitotic chromosome assembly in human cells. Mol Biol Cell 15, 3296–3308.
Orthwein A, Fradet-Turcotte A, Noordermeer SM, Canny MD, Brun CM, Strecker J, Escribano-Diaz C, Durocher D (2014). Mitosis inhibits DNA double-strand break repair to guard against telomere fusions. Science 344, 189–193.
Petersen J, Paris J, Willer M, Philippe M, Hagan IM (2001). The S. pombe aurora-related kinase Ark1 associates with mitotic structures in a stage dependent manner and is required for chromosome segregation. J Cell Sci 114, 4371–4384.
Petrova B, Dehler S, Kruitwagen T, Heriche JK, Miura K, Haering CH (2013). Quantitative analysis of chromosome condensation in fission yeast. Mol Cell Biol 33, 984–998.
Ponticelli AS, Smith GR (1989). Meiotic recombination-deficient mutants of Schizosaccharomyces pombe. Genetics 123, 45–54.
Renshaw MJ, Ward JJ, Kanemaki M, Natsume K, Nedelec FJ, Tanaka TU (2010). Condensins promote chromosome recoiling during early anaphase to complete sister chromatid separation. Dev Cell 19, 232–244.
Reyes C, Serrurier C, Gauthier T, Gachet Y, Tournier S (2015). Aurora B prevents chromosome arm separation defects by promoting telomere dispersion and disjunction. J Cell Biol 208, 713–727.
Rieder CL, Cole RW, Khodjakov A, Sluder G (1995). The checkpoint delaying anaphase in response to chromosome monoorientation is mediated by an inhibitory signal produced by unattached kinetochores. J Cell Biol 130, 941–948.
Rudner AD, Murray AW (1996). The spindle assembly checkpoint. Curr Opin Cell Biol 8, 773–780.
Sakuno T, Tada K, Watanabe Y (2009). Kinetochore geometry defined by cohesion within the centromere. Nature 458, 852–858.
Sampath SC, Ohi R, Leismann O, Salic A, Pozniakovski A, Funabiki H (2004). The chromosomal passenger complex is required for chromatin-induced microtubule stabilization and spindle assembly. Cell 118, 187–202.
Scherthan H (2001). A bouquet makes ends meet. Nat Rev Mol Cell Biol 2, 621–627.
Steigemann P, Wurzenberger C, Schmitz MH, Held M, Guizetti J, Maar S, Gerlich DW (2009). Aurora B-mediated abscission checkpoint protects against tetraploidization. Cell 136, 473–484.
Tada K, Susumu H, Sakuno T, Watanabe Y (2011). Condensin association with histone H2A shapes mitotic chromosomes. Nature 474, 477–483.
Tanaka TU, Rachidi N, Janke C, Pereira G, Galova M, Schiebel E, Stark MJ, Nasmyth K (2002). Evidence that the Ipl1-Sli15 (Aurora kinase-INCENP) complex promotes chromosome bi-orientation by altering kinetochore-spindle pole connections. Cell 108, 317–329.
Tomita K, Cooper JP (2007). The telomere bouquet controls the meiotic spindle. Cell 130, 113–126.
Tomonaga T, Nagao K, Kawasaki Y, Furuya K, Murakami A, Morishita J, Yuasa T, Sutani T, Kearsey SE, Uhlmann F, Nasmyth K, Yanagida M (2000). Characterization of fission yeast cohesin: essential anaphase proteolysis of Rad21 phosphorylated in the S phase. Genes Dev 14, 2757–2770.
Toth A, Ciosk R, Uhlmann F, Galova M, Schleiffer A, Nasmyth K (1999). Yeast cohesin complex requires a conserved protein, Eco1p(Ctf7), to establish cohesion between sister chromatids during DNA replication. Genes Dev 13, 320–333.
Tournier S, Gachet Y, Buck V, Hyams JS, Millar JB (2004). Disruption of astral microtubule contact with the cell cortex activates a Bub1, Bub3, and Mad3-dependent checkpoint in fission yeast. Mol Biol Cell 15, 3345–3356.
Uhlmann F, Lottspeich F, Nasmyth K (1999). Sister-chromatid separation at anaphase onset is promoted by cleavage of the cohesin subunit Scc1. Nature 400, 37–42.
Uhlmann F, Nasmyth K (1998). Cohesion between sister chromatids must be established during DNA replication. Curr Biol 8, 1095–1101.
Van Ly D, Low RRJ, Frolich S, Bartolec TK, Kafer GR, Pickett HA, Gaus K, Cesare AJ (2018). Telomere loop dynamics in chromosome end protection. Mol Cell 71, 510–525.e516.
Vanoosthuyse V, Prykhozhij S, Hardwick KG (2007). Shugoshin 2 regulates localization of the chromosomal passenger proteins in fission yeast mitosis. Mol Biol Cell 18, 1657–1669.
Vassetzky NS, Gaden F, Brun C, Gasser SM, Gilson E (1999). Taz1p and Teb1p, two telobox proteins in Schizosaccharomyces pombe, recognize different telomere-related DNA sequences. Nucleic Acids Res 27, 4687–4694.
Watanabe Y, Nurse P (1999). Cohesin Rec8 is required for reductional chromosome segregation at meiosis. Nature 400, 461–464.
Watanabe Y, Yokobayashi S, Yamamoto M, Nurse P (2001). Pre-meiotic S phase is linked to reductional chromosome segregation and recombination. Nature 409, 359–363.
Yamagishi Y, Honda T, Tanno Y, Watanabe Y (2010). Two histone marks establish the inner centromere and chromosome bi-orientation. Science 330, 239–243.
Yokobayashi S, Yamamoto M, Watanabe Y (2003). Cohesins determine the attachment manner of kinetochores to spindle microtubules at meiosis I in fission yeast. Mol Cell Biol 23, 3965–3973.